L. Kleeman, "Advanced Sonar and Odometry Error Modeling for Simultaneous Localisation and Map Building" Proceedings of the IEEE/RSJ International Conference on Intelligent Robots and Systems, Las Vegas 2003, pp 699-704.

Advanced Sonar and Odometry Error Modeling for Simultaneous Localisation and Map Building

Lindsay Kleeman
Intelligent Robotics Research Centre,
Department of Electrical and Computer Systems Engineering
Monash University, Australia
Lindsay.Kleeman@eng.monash.edu.au

***Abstract* - An advanced sonar sensor produces accurate range and bearing measurements, classifies targets and rejects interference with one sensing cycle. Two advanced sonar systems are used to simultaneously localise and map an indoor environment using a mobile robot. This paper presents the approach and results from on-the-fly map building using a Kalman filter and a new odometry error model that incorporates variations in effective wheel separation and angle measurements. This model is suited to pneumatic tyre odometry errors where the wheel separation has been found to vary unpredictably with floor surface and path curvature. The paper also presents techniques for detecting sonar feature clutter and selecting strong candidates for ultrasonic landmarks. The paper illustrates that sonar SLAM data association problems are significantly simplified when advanced sonar sensors are employed compared to Polaroid ranging modules.**

1. Introduction

Considerable research effort has been expended in producing sonar maps for localisation and navigation of indoor environments [1,2,3,4]. Almost all research has utilised sonar Polaroid Ranging Modules (PRM) or equivalent that provide range to the first sonar target. The PRM has presented significant obstacles to producing reliable maps due to the lack of target classification and bearing information. Classifying a feature as a point or line type allows prediction of measurements, allows simpler data association and is desirable for a coherent map. The lack of reliable bearing information makes data association and accurate feature location difficult. This paper presents an alternative approach to sonar map building and localisation where a high quality and accurate sonar sensor is deployed. The sonar systems are named "advanced sonar" to distinguish them from the PRM.

This paper presents new results of simultaneous localisation and map building (SLAM) employing on-the-fly advanced sonar measurements and two wheeled odometry. Previous work [4,6] using an earlier version of the sonar sensor required a stationary robot for sonar classification, which meant that measurements were taken at intervals of approximately one metre. Here the sonar sensors fire as the robot moves which results in more detailed maps. A new odometry model is introduced that extends previous work [7] and includes the effects of random perturbations in the effective wheel separation and is appropriate for robots with pneumatic wheels as in this work. Moreover a new approach is presented for automatic calibration of odometry, speed of sound and sonar positions on the robot.

The paper presents the specification of the advanced sonar and robot in section 2, the directed sensing strategy in section 3 and details of the SLAM approach in section 4. This section also includes the new odometry error model that extends [7]. An automated calibration procedure is briefly described in section 5 and results are discussed in section 6.

2 Advanced sonar specification and SLAMbot Configuration

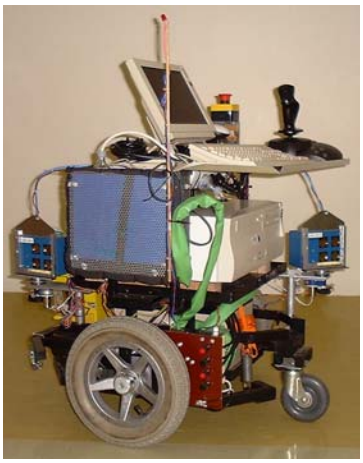

Figure 1 – SLAMbot with front and rear panning advanced sonar DSP based sensors.

The robot named SLAMbot is shown in Figure 1 and performs on-the-fly map building and localisation. SLAMbot is has front and rear advanced DSP sonar systems, two drive wheels with encoders that resolve to 0.5 mm and a wheel separation of 640 mm. The advanced sonar systems [8,9,4] report range, bearing and echo amplitudes out to 5 metres range with an error standard deviation of 0.2 mm and 0.1 degrees for strong reflectors such as walls. These errors depend on an accurate calibration of the speed of sound and calm air conditions. The sonar also classifies targets whilst the robot is moving

with a single measurement cycle of approximately 35 msec using nearly simultaneous firing of two transmitters. Classification types are planes, right-angled concave corners and edge reflectors. The sonar systems can smoothly rotate whilst sensing. The pan encoders resolve to 0.18 degrees. Interference between the sonar systems and from external sources is rejected using a double pulse scheme [9,10]. Sonar measurements are time stamped by the sensor to 1 msec resolution and the sensor clock is regularly synchronised to the host Linux computer clock to within 2 msecs using real time high priority threads.

3 Wipe directed sensing strategy

A simple directed sensing strategy is employed during mapping experiments. Each sonar sensor continuously pans forwards and backwards across its full angle range of 225 degrees at 60 deg/sec similar to a windscreen wiper. For the purposes of SLAM, the robot motion is controlled manually with a joystick.

3.1 Measurement Selection and Clutter

For each sonar cycle only one measurement is retained for reasons of simplicity and robustness. The maximum amplitude measurement is used since selects good ultrasonic landmarks. After each scan, sonar measurements are clustered based on target position compensated by odometry. A new measurement within a small difference to any one in a cluster under construction is included in the cluster. The maximum amplitude measurement of the cluster is then presented to the SLAM Extended Kalman filter. There are two reasons that *every* measurement is not processed by the Kalman filter: (i) sonar errors are highly correlated in time and space [10] and so little new information would be obtained from the same target and (ii) the processing time per measurement for SLAM cannot keep up with the sensor data rate.

Cluster statistics are kept to allow rejection of cluttered clusters that can cause incorrect associations in the Kalman filter. The statistics are the deviation in ranges and bearings referenced to the robot position at the start of the scan. The most common target type to encounter clutter is the edge, and is rejected when the range and bearing deviations exceed 2.5 mm per metre range or 0.2 degrees per metre range.

4 SLAM implementation

A Kalman filter based SLAM implementation is employed based on the description by Davison [11] where all map features are updated on each measurement step. There are many approaches reported [5,4,11,12,13] that speed up the update of the features and their covariances based on approximations and local map decompositions.

4.1 Robot state vector

The robot state represents the angle and position of the robot and the speed of sound as follows:

$$\mathbf{x} = \begin{bmatrix} \theta & x & y & c \end{bmatrix}^T \tag{1}$$

The position is referenced to the centre of the drive wheel axis. The speed of sound is estimated on-the-fly since it increases by about 0.5% per degree Celsius and is affected to a lesser extent by humidity and carbon dioxide levels. Over the duration of a SLAM mission the speed of sound can vary significantly.

4.2 Feature Representation

Three types of features are identified by the advanced sonar sensors – planes, concave corners and edges. The latter two types are represented by a two dimensional point (x_p, y_p). The plane feature is represented by a line with an angle ϕ and the minimum distance d to the global coordinate system origin as shown in Figure 2. A point on the line (ϕ, d) satisfies the parametric equation:

$$\begin{aligned} x &= d\cos\phi + t\sin\phi \\ y &= d\sin\phi + t\cos\phi \end{aligned} \tag{2}$$

where t is the signed distance from the nearest point on the line to the origin. The representation (ϕ, d) of a line has the alternative of $(\phi+\pi, -d)$ that results in the same parametric equations except t reverses sign. Here the two lines are considered different since they correspond to sensing from different sides of the line. The angle of the line always corresponds to the sonar sensing direction. If the line were sensed from the other side to the coordinate origin, a negative distance parameter would be recorded. Previous sonar mapping work [14] used the line representation (a, b) to represent a line with equation $ax+by=a^2+b^2$ as shown in Figure 2. This representation may become ill-conditioned when a lines passes nearby the origin.

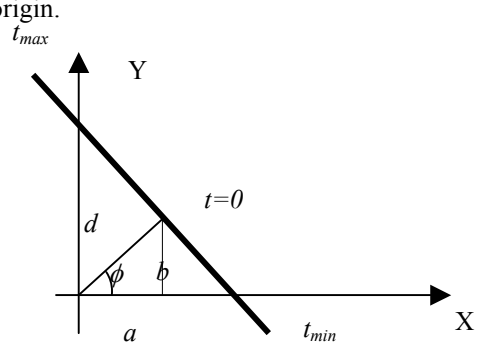

Figure 2 – Line representation

The extent of a line is represented by maximum and minimum t parameters t_{max} and t_{min} from equation (2).

New sonar measurements are only fused with the line if their t parameter lies in the interval $[t_{max}+ext,\ t_{min}-ext]$ where 0.4 metres has been chosen for *ext*.

Similarly point features represent an extent based on "viewing" angles which are restricted to less than a 90 degrees range per feature to account for the properties of corners and edges in practice. In particular the occurrence of corridor wall mouldings shown in Figure 3 are classified by the sonar as an edge. The moulding protrudes a centimetre from the wall which is not sufficient to allow the formation of a virtual image of the sonar transducers. Nevertheless these features are strong acoustic reflectors. By restricting a single feature to 90 degrees viewing angle, the left and right "edges" in Figure 3 are prevented from fusing in the SLAM algorithm. To help with maintenance of map features, the number of sensor measurements associated with a feature is recorded along with the times of these measurements. This can be referenced to an array of times linked to robot poses.

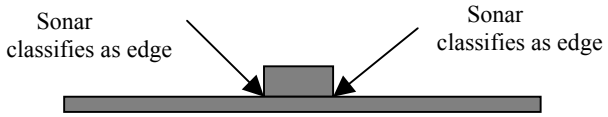

Figure 3 – Plan view of a wall mouldings classified as a sonar edge.

4.3 Odometry error model

The robot odometry estimate of robot pose at time step *k+1* is determined using the following [7] equations:

$$\begin{aligned}\mathbf{x}(k) &\equiv \begin{bmatrix}\theta(k) & x(k) & y(k)\end{bmatrix}^T \\ \mathbf{y}(k) &\equiv \begin{bmatrix}L_R(k) & L_L(k) & B\end{bmatrix}^T \\ \mathbf{x}(k+1) &= \mathbf{x}(k) + \mathbf{f}(\mathbf{x}(k), \mathbf{y}(k))\end{aligned} \tag{3}$$

$$\mathbf{f}(\mathbf{x}(k), \mathbf{y}(k)) = \begin{bmatrix} \frac{L_R - L_L}{B} \\ \frac{L_R + L_L}{2}\cos\left(\theta(k) + \frac{L_R - L_L}{2B}\right) \\ \frac{L_R + L_L}{2}\sin\left(\theta(k) + \frac{L_R - L_L}{2B}\right) \end{bmatrix} \tag{4}$$

where at time step *k*, $\theta(k)$ is the robot heading angle, and $x(k)$ and $y(k)$ are the x and y coordinates of the centre of the robot wheel axis. The error model adopted here assumes the error sources are additive white noise on the wheel separation, B, and the left and right wheel length measurements, L_L and L_R. This work extends previous work [7] that considers noise on L_L and L_R alone. The robot employed in the current work has wide inflatable tyres that provide good traction at the expense of wheel separation variation. Calibration experiments have shown that the effective wheel separation varies with floor surface and path curvature in an unpredictable manner. Using a first order Taylor expansion of equations (3,4) the iterative equation can be derived in terms of the Jacobians $\frac{\partial \mathbf{f}}{\partial \mathbf{x}}$ and $\frac{\partial \mathbf{f}}{\partial \mathbf{y}}$:

$$\Delta\mathbf{x}(k+1) \cong \left(\mathbf{I} + \frac{\partial \mathbf{f}}{\partial \mathbf{x}}\right)\Delta\mathbf{x}(k) + \frac{\partial \mathbf{f}}{\partial \mathbf{y}}\Delta y(k) \tag{5}$$

where

$$\mathbf{I} + \frac{\partial \mathbf{f}}{\partial \mathbf{x}} = \begin{bmatrix} 1 & 0 & 0 \\ -L\sin\theta & 1 & 0 \\ L\cos\theta & 0 & 1 \end{bmatrix} \tag{6}$$

$$\frac{\partial \mathbf{f}}{\partial \mathbf{y}} = \begin{bmatrix} \frac{1}{B} & -\frac{1}{B} & -\frac{D}{B} \\ \frac{\cos\theta}{2} - \frac{L\sin\theta}{B} & \frac{\cos\theta}{2} + \frac{L\sin\theta}{B} & \frac{D.L}{2B}\sin\theta \\ \frac{\sin\theta}{2} + \frac{L\cos\theta}{B} & \frac{\sin\theta}{2} - \frac{L\cos\theta}{B} & -\frac{D.L}{2B}\cos\theta \end{bmatrix} \tag{7}$$

$$L = \tfrac{L_R + L_L}{2} \quad D = \tfrac{L_R - L_L}{B} \quad \theta = \theta(k) + \tfrac{L_R - L_L}{2B} \tag{8}$$

The covariance of the error in the robot pose at step *k+1* is now derived in terms of step *k*:

$$\begin{aligned}\mathbf{P}(k+1) &\equiv E\left\langle \Delta\mathbf{x}(k+1)\Delta\mathbf{x}(k+1)^T \right\rangle \\ &= \left(\mathbf{I} + \frac{\partial \mathbf{f}}{\partial \mathbf{x}}\right) E\left\langle \Delta\mathbf{x}(k)\Delta\mathbf{x}(k)^T \right\rangle \left(\mathbf{I} + \frac{\partial \mathbf{f}}{\partial \mathbf{x}}\right)^T \\ &\quad + \frac{\partial \mathbf{f}}{\partial \mathbf{y}} E\left\langle \Delta y(k)\Delta y(k)^T \right\rangle \frac{\partial \mathbf{f}}{\partial \mathbf{y}}^T \\ &= \underbrace{\mathbf{P}(k) + \mathbf{P}(k)\frac{\partial \mathbf{f}}{\partial \mathbf{x}}^T + \frac{\partial \mathbf{f}}{\partial \mathbf{x}}\mathbf{P}(k) + \frac{\partial \mathbf{f}}{\partial \mathbf{x}}\mathbf{P}(k)\frac{\partial \mathbf{f}}{\partial \mathbf{x}}^T}_{\text{covariance propagation}} \\ &\quad + \underbrace{\frac{\partial \mathbf{f}}{\partial \mathbf{y}}\mathbf{Q}(k)\frac{\partial \mathbf{f}}{\partial \mathbf{y}}^T}_{\text{new error}}\end{aligned} \tag{9}$$

where E is expectation and $\mathbf{Q}(k)$ is the error covariance of $\mathbf{y}(k)$, the wheel measurements and separation. Note that in equation (9) the errors in robot pose, $\mathbf{x}$, at time k and the new errors in odometry parameters $\mathbf{y}$ at time k are assumed to be independent. The 4 terms involving $\mathbf{P}(k)$ in the equation (9) can be reduced to the following equations that are efficient to implement:

$$
\begin{aligned}
p'_{33}(k+1) &= p_{33}(k) + 2L.c.p_{31}(k) + L^2c^2p_{11}(k) \\
p'_{23}(k+1) &= p'_{32}(k+1) = p_{23}(k) + L.c.p_{12}(k) \\
&\quad - L.s.p_{31}(k) - L^2s.c.p_{11}(k) \\
p'_{22}(k+1) &= p_{22}(k) - 2L.s.p_{12}(k) + L^2s^2p_{11}(k) \\
p'_{13}(k+1) &= p'_{31}(k+1) = p_{13}(k) + L.c.p_{11}(k) \\
p'_{12}(k+1) &= p'_{21}(k+1) = p_{12}(k) - L.s.p_{11}(k) \\
p'_{11}(k+1) &= p_{11}(k)
\end{aligned}
\tag{10}
$$

where **P**= [p_{ij}] and $c=cos(\theta)$ and $s=sin(\theta)$. Note that if the above equations are implemented in the order shown, the covariance entries can be update in situ. The primes (') indicate that the remaining term involving **Q**(k) in equation (9) needs to be included before the final covariance **P** is obtained. The errors in L_R, L_L and B are assumed to be independent:

$$
Q = \begin{bmatrix} \sigma_R^{\,2} & 0 & 0 \\ 0 & \sigma_L^{\,2} & 0 \\ 0 & 0 & \sigma_B^{\,2} \end{bmatrix} \tag{11}
$$

Expanding the final term in equation (9) results in the covariance update equations:

$$
\begin{aligned}
p_{11}(k+1) &= p'_{11}(k+1) + \frac{\sigma_R^{\,2}}{B^2} + \frac{\sigma_L^{\,2}}{B^2} + \frac{D^2}{B^2}\sigma_B^{\,2} \\
p_{12}(k+1) &= p'_{12}(k+1) + \left(\frac{c}{2B} - \frac{L.s}{B^2}\right)\sigma_R^{\,2} \\
&\quad - \left(\frac{c}{2B} + \frac{L.s}{B^2}\right)\sigma_L^{\,2} - \frac{D^2L.s}{2B^2}\sigma_B^{\,2} \\
p_{13}(k+1) &= p'_{13}(k+1) + \left(\frac{s}{2B} + \frac{L.c}{B^2}\right)\sigma_R^{\,2} \\
&\quad - \left(\frac{s}{2B} - \frac{L.c}{B^2}\right)\sigma_L^{\,2} + \frac{D^2L.c}{2B^2}\sigma_B^{\,2} \\
p_{22}(k+1) &= p'_{22}(k+1) + \left(\frac{c}{2} - \frac{L.s}{B}\right)^2\sigma_R^{\,2} \\
&\quad + \left(\frac{c}{2} + \frac{L.s}{B}\right)^2\sigma_L^{\,2} + \left(\frac{D.L.s}{2B}\right)^2\sigma_B^{\,2} \\
p_{23}(k+1) &= p'_{23}(k+1) + \left(\frac{c}{2} - \frac{L.s}{B}\right)\left(\frac{s}{2} + \frac{L.c}{B}\right)\sigma_R^{\,2} \\
&\quad + \left(\frac{c}{2} + \frac{L.s}{B}\right)\left(\frac{s}{2} - \frac{L.c}{B}\right)\sigma_L^{\,2} - \left(\frac{D.L}{2B}\right)^2 s.c.\sigma_B^{\,2} \\
p_{33}(k+1) &= p'_{33}(k+1) + \left(\frac{s}{2} + \frac{L.c}{B}\right)^2\sigma_R^{\,2} \\
&\quad + \left(\frac{s}{2} - \frac{L.c}{B}\right)^2\sigma_L^{\,2} + \left(\frac{D.L.c}{2B}\right)^2\sigma_B^{\,2}
\end{aligned}
\tag{12}
$$

How are values determined for the variance $\sigma_R^{\,2}, \sigma_L^{\,2}$ and $\sigma_B^{\,2}$? For a given distance or angle change, the final covariance should be independent of the number of steps to traverse a path. To find a value for $\sigma_B^{\,2}$, consider the p_{11} (ie angle variance) additive term in the above equation when $\sigma_R^{\,2} = \sigma_L^{\,2} = 0$. This term must be proportional to the absolute value of the angle change D in order to produce a consistent sum for different step sizes. Therefore a proportionality constant k is introduced to give:

$$
\frac{D^2}{B^2}\sigma_B^{\,2} = k|D| \Rightarrow \sigma_B^{\,2} = \frac{k.B^2}{|D|} \tag{13}
$$

Let A be the angle error standard deviation introduced by noise on the wheel separation parameter B for a full 2π revolution of the robot in one step, then

$$
\frac{(2\pi)^2}{B^2}\frac{k.B^2}{2\pi} = A^2 \Rightarrow k = \frac{A^2}{2\pi} \quad and \quad therefore \quad \sigma_B^{\,2} = \frac{A^2B^2}{2\pi|D|} \tag{14}
$$

Values for $\sigma_R^{\,2}$ and $\sigma_L^{\,2}$ must be proportional to L at each step so that the total contribution of error along the path is dependent only on the path not the number of steps. To accumulate a standard deviation error E from 1 metre of travel,

$$
\sigma_R^{\,2} = E^2|L_R| \quad and \quad \sigma_L^{\,2} = E^2|L_L| \tag{15}
$$

Despite the apparent complexity of the covariance update equations (12), they are straightforward to implement and the C++ code to update the odometry pose and covariance runs in under 5 usec on a 850 MHz Pentium. This represents about 0.5 % computational loading since the odometry estimate and error covariance is updated every 10 msec.

4.4 Sonar error covariance model

The sonar error model estimates the covariance of errors in sonar range and bearing measurements. The error model depends on the feature type. Measurement of edges are less reliable than plane and corner feature types, due to two factors: (i) reduced echo amplitude and (ii) clutter is more common. Therefore a more conservative error model is adopted for edge features. The range and bearing measurements are assumed to be independent [15]. The sonar error model needs to take into consideration vibrations and swaying of the robotic platform that are not seen by odometry. These errors can be significant compared to the stationary robot errors and the sonar model adopted is necessarily conservative:

$$
\begin{aligned}
\mathbf{z} &= [angle(radians) \quad TOF(seconds)]^T \\
\mathbf{R} &= scale * \begin{bmatrix} (1.0degree \times \frac{\pi}{180})^2 & 0 \\ 0 & (2 \times 0.002\, metres\ range/c)^2 \end{bmatrix}
\end{aligned}
\tag{16}
$$

where *scale* is *maximum{1,range(in metres)}* for edges and *1* for corners and planes.

4.5 Measurement to Feature Association

New measurements can either generate a new map feature or be fused to existing map features. In the latter case the measurement improves the robot pose and the accuracy of the feature pose and possibly increases the extent of the feature. In the Kalman filter all error covariance and cross covariance matrices are affected by the fusion of a measurement and the processing complexity of the operation increases with n^2 unless the map is divided into submaps [5,4,13].

The decision of which feature, if any, a measurement should be fused with is called the association problem. Incorrect associations can cause gross errors in the map and even divergence of SLAM. Failure to associate a measurement with its genuine feature results in suboptimal robot localisation and feature errors and possibly the duplication or shadowing of future map features displaced in position and angle. Association must satisfy:

1. The feature and measurement classifications agree (ie plane, corner or edge)
2. The length of a line is extended by less than 0.4 metres.
3. For a point feature, the viewing angle to the centre of previous viewing angles is less than 30 degrees.
4. The measurement satisfies a standard validation gate condition for a Kalman filter [14] for one and only one feature.

If one of the conditions 1, 2 or 3 are not satisfied and the measurement does not fall into any validation gate, a new feature is initiated. If the measurement falls into more than one feature's validation gate, the measurement is ignored.

5 Calibration of Odometry and Sonar

The pneumatic tyres require odometry calibration to be performed frequently. Calibration of the sonar position in the robot coordinate frame and the speed of sound is a by-product of this technique. Sonar and odometry measurements are collected for a robot maneuver that allows both sonar sensors to observe a dozen uncluttered features over a few minutes with the robot moving forward turning and retracing its path several times as shown in Figure 4. In order to determine the speed of sound and provide a distance reference for odometry, the distance between two parallel planes is measured and used as a constraint during minimisation of a cost function. The cost function is the sum of square differences between expected measurements and real measurements based on average feature positions and odometry. Special care is taken in choosing the form of the parameters and their order to decouple the minimisation of cost between parameters. For example c is optimised first since this affects sonar features perpendicular to robot motion, and then $(R_R+R_L)/c$ which affects features in line with robot motion only. Other parameters of odometry and sonar follow:

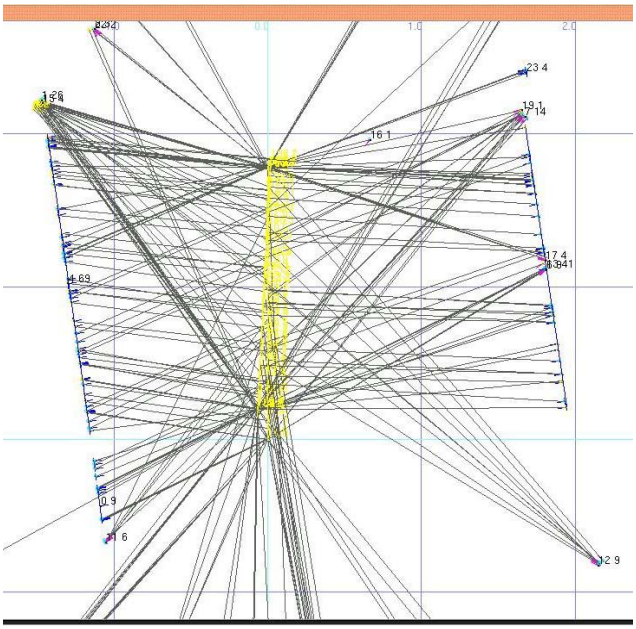

Figure 4 – The robot map data used for calibration of odometry, speed of sound and sonar pose on the robot.

6 Results

Figures 4 and 5 show the results of SLAM experiments where the robot was travelling at less than 0.1 m/s in order to produce dense maps. These maps can be processed in real time since less than 200 features typically are present. Measurement innovations produced by the Kalman filter are usually less than a 0.01 m and 0.01 radians except when features not seen for a considerable time are encountered. In figure 5, phantom features are observed outside the physical corridor due to multi-path echoes. These do not present a problem for SLAM unless the map is used for navigation. In that case techniques exist to allow detection of these features [6].

7 Conclusions and Future Work

Two advanced sonar systems combined with a new odometry error model have been shown to produce high quality sonar feature maps with a Kalman filter SLAM approach. This work highlights the benefits of accurate and appropriate sensor information that circumvents higher level sophisticated hypothesis formation over extended time periods that is necessary to associate and classify with conventional Polaroid ranging module sonar

[3]. The advanced sonar allows reliable measurement association with map features. Nevertheless the association can fail when odometry errors exceed expectations or linearisation errors accumulate as reported in [2] and future work will concentrate on improving association and recovering from failure of SLAM. The related problems of loop closure and laser sonar fusion will also be investigated.

References

[1] T Tsubouchi; "Nowadays trends in map generation for mobile robots" IROS 96, pp: 828 –833.
[2] G Zunino,; H Christensen,. "Simultaneous localization and mapping in domestic environments" Int. Conf. Multisensor Fusion and Integration for Intelligent Systems, 2001. pp: 67- 72.
[3] H. J. S. Feder, J. J. Leonard and C. M. Smith. "Adaptive mobile robot navigation and mapping." IJRR, July 1999 pp. 650-668.
[4] J.J Leonard, H.J.S. Feder, "Decoupled stochastic mapping for mobile robot & AUV navigation" IEEE J. Oceanic Eng., Vol.26, Iss.4, 2001 pp:561-571
[5] K S Chong and L. Kleeman, "Feature-based mapping in real, large scale environments using an ultrasonic array", IJRR, 1999, pp. 3-19.
[6] K S Chong and L Kleeman, "Sonar based map building for a mobile robot", ", IEEE Int Conf Robotics & Automation, 1997, pp. 1700-1705.
[7] K S Chong and L Kleeman, "Accurate odometry and error modelling for a mobile robot", IEEE Int Conf Robotics & Automation, 1997, pp. 2783-2788.
[8] L. Kleeman, "On-the-fly classifying sonar with accurate range and bearing estimation" IROS 2002, pp.178-183.
[9] A. Heale and L. Kleeman, "Fast target classification using sonar" IROS 2001, p 1446-1451.
[10] L. Kleeman, "Fast and accurate sonar trackers using double pulse coding", IROS 99, pp.1185-1190.
[11] A Davison, Mobile Robot Navigation Using Active Vision D.Phil Thesis University of Oxford, 1998.
[12] M Montemerlo, and S Thrun, and D Koller and B Wegbreit, "FastSLAM: A Factored Solution to the Simultaneous Localization and Mapping Problem", 2002, Proc. of the AAAI National Conf Artificial Intelligence, Edmonton, Canada.
[13] J Guivant, E Nebot "Improving Computational and Memory Requirements of Simultaneous Localization and Map Building Algorithms" Proc 2002 IEEE Int. Conf Robotics & Automation 2002, pp. 2731-2736.
[14] K S Chong and L. Kleeman, "Mobile robot map building for an advanced sonar array and accurate odometry", IJRR 1999, pp. 20-36
[15] L. Kleeman and R. Kuc, "Mobile robot sonar for target localization and classification", IJRR 1995, pp 295-318.

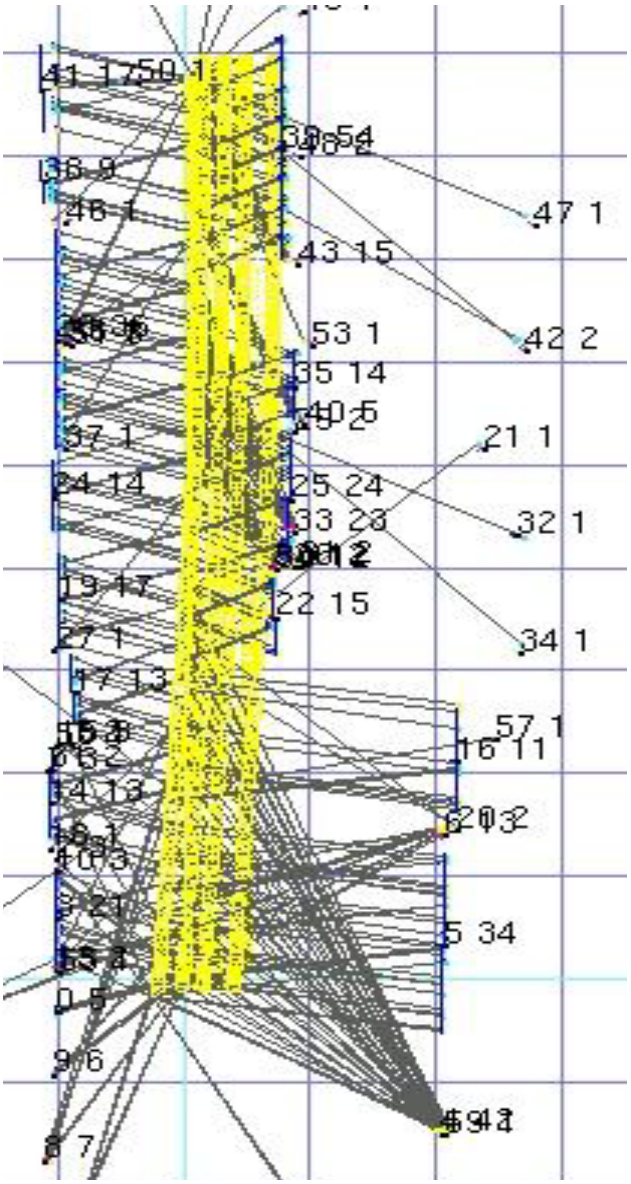

Figure 5 – Map and measurements for a corridor where the robot travels up 9 metres turns and travels back to the start point. Map features are labelled with a sequence number and number of associations. Measurement are indicated by a line from the robot position to the measurement point.